Journal of

Mechanics of Materials and Structures

LIMIT ANALYSIS OF CLOISTER VAULTS: THE CASE STUDY OF PALAZZO CARACCIOLO DI AVELLINO

Antonio Gesualdo, Giuseppe Brandonisio, Antonello De Luca, Antonino Iannuzzo, Andrea Montanino and Carlo Olivieri

Volume 14, No. 5 December 2019

msp

JOURNAL OF MECHANICS OF MATERIALS AND STRUCTURES
Vol. 14, No. 5, 2019
dx.doi.org/10.2140/jomms.2019.14.739

LIMIT ANALYSIS OF CLOISTER VAULTS: THE CASE STUDY OF PALAZZO CARACCIOLO DI AVELLINO

ANTONIO GESUALDO, GIUSEPPE BRANDONISIO, ANTONELLO DE LUCA, ANTONINO IANNUZZO, ANDREA MONTANINO AND CARLO OLIVIERI

The equilibrium of cloister masonry vaults, treated as composed of unilateral material in the sense of Heyman, is the topic of the present work. For such a material, the safe and the kinematic theorems of limit analysis can be employed to detect equilibrium and nonequilibrium. In the spirit of the safe theorem, the structure is stable if a statically admissible stress field can be detected. On allowing for singular stresses, here we consider statically admissible stress fields concentrated on surfaces or lines lying inside the masonry vault. Such structures are unilateral membranes, whose geometry is described a la Monge, and the equilibrium of them is formulated in Pucher form, that is, in terms of the so-called projected stresses over the planform Ω. The problem, under purely parallel loads, is reduced to a single partial differential equation of the second-order, in two space variables, where the shape function f and the stress function F appear symmetrically. The unilateral restrictions require that the membrane surface S lies in between the extrados and intrados surfaces of the vault and that the stress function be concave. In the present work, by starting with a sensible choice of a concave stress function F, the transverse equilibrium equation is solved for f by imposing suitable boundary conditions. A cloister vault of *Palazzo Caracciolo di Avellino*, a XIV century building located along *via dell'Anticaglia* in Naples, is the case study. For two load conditions, membrane surfaces and geometrical safety factors are identified.

1. Introduction

The present work is concerned with the equilibrium of cloister masonry vaults, treated as composed of no-tension material in the sense of Heyman [1966]. For such a material the safe and the kinematic theorems of limit analysis can be employed to detect equilibrium and nonequilibrium, as originally shown in [Heyman 1966; Kooharian 1952; Livesley 1978] and most recently in [Como 1992; Angelillo 2015; 2019; Gesualdo et al. 2017; 2019; Angelillo et al. 2010; 2014; 2016; 2018; Fortunato et al. 2014; 2016; 2018; Brandonisio et al. 2013; 2015; Iannuzzo et al. 2018a; 2018c; 2018b].

The method that we apply here is the so-called membrane equilibrium analysis (MEA), originated in the papers on vaults [Angelillo and Fortunato 2004; Fraternali 2010; Fraternali et al. 2002; Angelillo et al. 2013]. The MEA can be seen as the continuous counterpart of the method called thrust network analysis, first proposed in a pioneering work by O'Dwyer [1999], and then developed in subsequent works in [Block et al. 2006; Block and Lachauer 2014; Vouga et al. 2012; De Goes et al. 2013; Miki et al. 2015; Marmo and Rosati 2017].

Keywords: limit analysis, vaults, masonry-like materials, Airy's stress function.

The classical Heyman hypotheses of null tensile strength, infinite compressive strength and no-sliding are the basis of the present approach, together with the static theorem of limit analysis. Statically admissible singular stress fields, in the form of surface and line Dirac deltas applied on material surfaces and lines are involved. The support lines Γ and surfaces S of these Dirac deltas can be interpreted as arches and membranes enclosed inside the vault thickness.

The unilateral assumption implies that the generalized stress on S be compressive, and restrict S to be located in between the extrados and intrados surfaces of the vault. Then, as in the case of the thrust line Γ that we can devise inside a plane arch, the ideal structure S is not fixed, but forms inside the masonry, in order to balance and transmit the external loads.

In the present paper, we essentially use the ideas put forward in [Angelillo and Fortunato 2004; Angelillo et al. 2013; Heyman 2012], by applying the method to cloister vaults of different geometry. The geometry of the membrane is described by means of a Monge representation and the equilibrium is expressed in Pucher form (see [Pucher 1934]). In this paper, by starting with a sensible choice of a restricted class of concave stress functions, the transverse equilibrium equation is solved for the shape by imposing suitable boundary conditions. In the flat part of the cloister vault, for example, the stress function F is considered quadratic because the projected stress is assumed constant. The case study of the cloister vaults of Palazzo Caracciolo di Avellino (an historical palace of Naples, whose basal part was built in the XIV century) is considered. Geometrical safety factors are computed for different cases of loading.

2. Mathematical preliminaries: Pucher stress

We study the equilibrium, under the action of given loads, of a membrane surface S contained inside the thickness of the shell.

The formulation of membrane equilibrium that we consider is essentially the one proposed by Pucher in his seminal paper [Pucher 1934], though here a more modern and straightforward formalism is adopted. The symmetry of the problem with respect to the two numeric functions of two variables controlling the shape and the stress is exploited by interchanging the role of data and unknowns with the aim of generating shapes for given stresses.

2.1. ***Geometry.*** The particular geometry of typical shells and domes allows for the representation, in Monge form, of a membrane surface S contained inside the structure, that is (see Figure 1)

$$\boldsymbol{x} = x_1 \hat{\boldsymbol{e}}_1 + x_2 \hat{\boldsymbol{e}}_2 + f(x_1, x_2)\, \hat{\boldsymbol{e}}_3, \tag{1}$$

where $\boldsymbol{x}$ is the position vector of points of S, $\{\hat{\boldsymbol{e}}_1, \hat{\boldsymbol{e}}_2, \hat{\boldsymbol{e}}_3\}$ is the orthonormal triad coherent with a given Cartesian frame $\{O;\ x_1, x_2, x_3\}$, the couple (x_1, x_2) belongs to a region Ω of the plane $\{O;\ x_1, x_2\}$ called planform of S, and $f = f(x_1, x_2)$ is a smooth function of its arguments. Summation convention over repeated indices will be used throughout these notes, implying that Greek indices range over 1, 2 and Latin indices over 1, 2, 3.

2.2. ***Forces and equilibrium.*** We consider the equilibrium of S subject to a given, possibly nonuniform, load $\boldsymbol{p}$ per unit projected area of S:

$$\boldsymbol{p} = -p\, \hat{\boldsymbol{e}}_3. \tag{2}$$

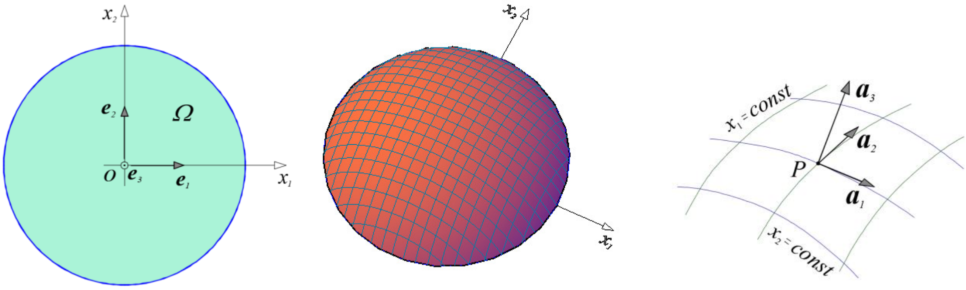

Figure 1. Monge representation of the membrane surface S of a spherical dome. Planform Ω (left), 3D view with curvilinear coordinates (x_1, x_2) (middle), and base vectors on S (right).

Calling $\boldsymbol{T}$ the generalized surface stress (that is, the stress per unit length on S), that is, the membrane stress on S, we can express it in the form

$$\boldsymbol{T} = T^{\alpha\beta}\boldsymbol{a}_\alpha \otimes \boldsymbol{a}_\beta, \tag{3}$$

$T^{\alpha\beta}$ being the contravariant components of $\boldsymbol{T}$ in the covariant base $\{\boldsymbol{a}_1, \boldsymbol{a}_2\}$ associated to the curvilinear coordinates (x_1, x_2) (see Figure 1). The pseudostresses $S_{\alpha\beta}$ (Pucher-stresses) can be introduced:

$$S_{\alpha\beta} = JT^{\alpha\beta}, \tag{4}$$

J being the ratio between the area on S and the corresponding projected area.

On introducing the stress potential F:

$$S^{11} = F_{,22}, \quad S^{22} = F_{,11}, \quad S^{12} = S^{21} = -F_{,12}, \tag{5}$$

the equilibrium problem is reduced to a single scalar equation in the unknown stress potential function F:

$$F_{,22}\, f_{,11} + F_{,11}\, f_{,22} - 2F_{,12}\, f_{,12} - p = 0. \tag{6}$$

The boundary condition for this partial differential equation can be either of the Dirichlet or of the Neumann type, that is,

$$F|_{\partial\Omega} = m, \quad \text{or} \quad \left.\frac{dF}{dn}\right|_{\partial\Omega} = -n, \tag{7}$$

or of any combination of the two on a partition of the boundary $\partial\Omega$.

2.3. ***Unilateral membranes and singular stresses.*** In the present study, we consider shells that are purely compressed under the effect of the loads. Then we assume that the generalized stress $\boldsymbol{T}$ is negative semidefinite: $\boldsymbol{T} \in \mathrm{Sym}^-$.

The first application of Pucher's transformation for compressed masonry vaults can be found in [Angelillo and Fortunato 2004], where it is shown that, due to the compression constraint, the matrix of the projected stress components $S^{\alpha\beta} = JT^{\alpha\beta}$ must be also negative semidefinite. In terms of the stress function F, this condition transforms into

$$F_{,11} + F_{,22} \leq 0, \quad F_{,11}\, F_{,22} - F_{,12}\, F_{,12} \geq 0, \tag{8}$$

hence, the surface described by $F(x_1, x_2)$ must be concave.

We admit that $F(x_1, x_2)$ be only continuous, that is, F may be folded. In this case the projected stress is a line Dirac delta with support along the projection Γ of the fold. The *Hessian* $\boldsymbol{H}$ of F is singular transversely to Γ, that is, it has a uniaxial singular part parallel to the unit vector $\boldsymbol{h}$ normal to Γ. Correspondingly the directional derivative of F in the direction of $\boldsymbol{h}$, called F_h, presents a jump. Therefore, the singular part of the Hessian $\boldsymbol{H}$ of F can be written as

$$\boldsymbol{H}_s = \delta(\Gamma)\, F_h\, \boldsymbol{h} \otimes \boldsymbol{h}, \tag{9}$$

$\delta(\Gamma)$ being the unit line Dirac delta on Γ. Analogously, the singular part of the corresponding projected stress (2) is a Dirac delta on Γ:

$$\boldsymbol{T}_s = \delta(T)\, F_h\, \boldsymbol{k} \otimes \boldsymbol{k}, \tag{10}$$

$\boldsymbol{k}$ being the unit vector tangent to Γ. The concavity of F implies the concavity of the fold, then F_h is negative and the corresponding projected singular stress concentrated on Γ is compressive.

3. Equilibrium of cross and cloister vaults

The simplified equilibrium solution of a cross vault can be easily devised through the so-called slicing technique (see [Heyman 1995]). The vault is sliced into strips parallel to the boundary arches and meeting along the cross diagonals; such strips carry the load per unit area and transfer it as a load per unit length to two diagonal cross arches discharging it as a vertical and horizontal load thrust to the four columns (see Figure 2, left). The analytical MEA version of this simplified geometrical approach can be found in [Angelillo and Fortunato 2004; Contestabile et al. 2016].

The slicing technique, that is, a method to reduce a 3D problem to a plane analysis, is applied to cloister vault (for a discussion on the slicing method, see [Angelillo et al. 2013; Bloch and Ochsendorf 2007; Como 2013; Fang et al. 2019]). A schematic view of the planform of a typical cloister vault is depicted in Figure 2 (right). Indeed, in this case, the slices should be taken orthogonally to the flat boundary, but if these elementary arches are interrupted along the cross diagonals, they transfer to them a load that pushes these cross arches upward, which means the concentrated force along them must be tensile. If instead these parallel arches are not interrupted and are allowed to cross each other, they must be fitted, in their central part, within two flat parallel boundaries (see Figure 2, right), a condition that, to be satisfied, requires a large thickness in the upper 1/3 of the vault.

In order to optimize the equilibrium solution, we propose to slice the vault with nonparallel arches in the lower 2/3 of the vault, making the arches cross each other in the upper central part (see Figure 3, left). The mathematical construction through MEA of such equilibrium state is described in the following paragraphs.

3.1. ***Equilibrium on the planform.*** To generate an equilibrium state of compression into the vault, we start from the assumption of a particular equilibrated stress regime in the planform, corresponding to the partition of the planform into zones of uniaxial and biaxial stress fields (see Figure 3, left). Referring

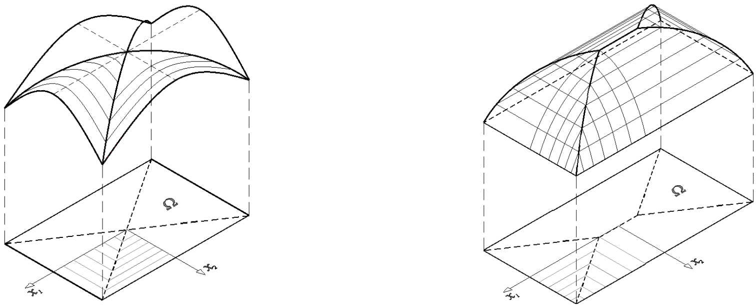

Figure 2. Slicing technique for simplified equilibrium solutions for cross vaults (left) and cloister vaults (right).

to this last figure for notations, Ω_2 is the uniaxial zone and Ω_1 is the zone where the projected stress is an uniaxial stress field along the directions of the segments reported pictorially in the figure. By calling $\pi/2-\alpha$ the angle that each ray forms with the straight external boundary, in each of the four wedges forming the region Ω_2 the fan of these rays of uniaxial compression can be given, as a one-parameter family of directions in terms of an abscissa x specified along the boundary, as

$$\tan\alpha = g(x), \tag{11}$$

the function $g(x)$ being fixed in advance and x is the length along the boundary.

We introduce, in the wedge Ω_{21} (see Figure 3, right), and similarly in the other outer lower regions Ω_{2j}, a curvilinear reference system $\{\vartheta^1 = x,\ \vartheta^2 = y\}$ with the curvilinear lines (that are actually straight lines) directed as the rays:

$$x_1 = x + y\,g(x), \quad x_2 = y, \tag{12}$$

where x_1, x_2 are the coordinates in Ω_{21}.

The natural base vectors $\boldsymbol{b}_1$ and $\boldsymbol{b}_2$ tangent to the $\{\vartheta^1, \vartheta^2\}$ curvilinear lines, denoting with a prime differentiation of numeric functions with respect to their argument, in Cartesian components in the reference (see Figure 3, right), are

$$\boldsymbol{b}_1 = \big(1 + y\,g'(\boldsymbol{x})\big)\,\hat{\boldsymbol{e}}_1, \quad \boldsymbol{b}_2 = g(x)\,\hat{\boldsymbol{e}}_1 + \boldsymbol{e}_2, \tag{13}$$

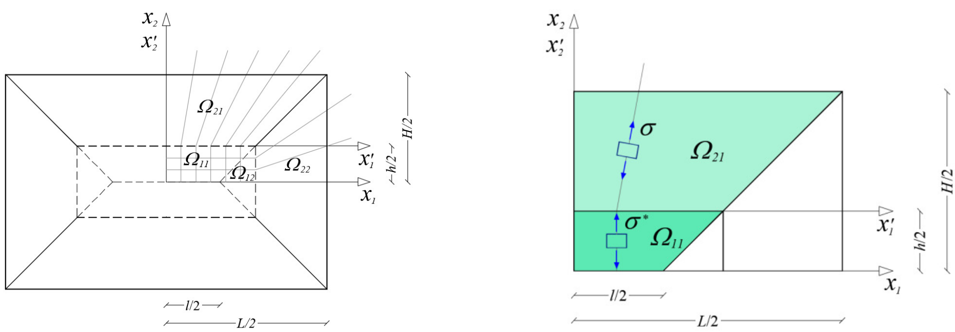

Figure 3. Partition of the planform into uniaxial and biaxial stress zones (left) and axial stress along the rays (right).

$\{\hat{\boldsymbol{e}}_1, \hat{\boldsymbol{e}}_2\}$ being the orthonormal pair coherent with the given Cartesian frame. We also consider the dual base vectors

$$\boldsymbol{b}^1 = \frac{1}{1 + y\, g'(\boldsymbol{x})}\hat{\boldsymbol{e}}_1 - \frac{g(x)}{1 + y\, g'(\boldsymbol{x})}\hat{\boldsymbol{e}}_2, \quad \boldsymbol{b}^2 = \hat{\boldsymbol{e}}_2. \tag{14}$$

The uniaxial projected stress in the fan zone can be written as

$$\boldsymbol{S} = s\, \boldsymbol{b}_2 \otimes \boldsymbol{b}_2, \tag{15}$$

s being the sole nonvanishing contravariant component of the projected stress in the curvilinear reference $\{\vartheta^1, \vartheta^2\}$. For the two equilibrium equations (12) to be satisfied, it must be

$$s = \frac{q(x)}{1 + y\, g'(\boldsymbol{x})}, \tag{16}$$

$q(x)$ being an arbitrary function of x, to be specified through the boundary conditions.

Calling $\hat{\boldsymbol{k}}$ the unit vector directed as $\boldsymbol{b}_2$, the physical stress component σ of this uniaxial stress field can be obtained as

$$\sigma = \boldsymbol{S} \cdot \hat{\boldsymbol{k}} \otimes \hat{\boldsymbol{k}}, \tag{17}$$

that is,

$$\sigma = -\frac{q(x)}{1 + y\, g'(\boldsymbol{x})}(1 + g^2(\boldsymbol{x})). \tag{18}$$

The emerging stress vector at the interface is then

$$\boldsymbol{t} = (\sigma \hat{\boldsymbol{k}} \otimes \boldsymbol{k})(-\hat{\boldsymbol{e}}_2) = q(x)\, g(x)\, \hat{\boldsymbol{e}}_1 + q(x)\, \hat{\boldsymbol{e}}_2. \tag{19}$$

The biaxial state in the central zone Ω_1 is produced by the superposition of two orthogonal uniaxial stress fields directed as the Cartesian axes. The kink of the compression rays at the straight interface $(y = 0)$ corresponds to a jump of the tangential component of stress producing a concentrated uniaxial stress of the form (21) along such interface.

The axial force $F_h(x)$ along the interface can be obtained by writing the equilibrium equation

$$F_h'(x) - q(x)\, g(x) = \boldsymbol{0}. \tag{20}$$

Instead, the normal component of the stress vector emerging at the interface is transmitted to the part Ω_{11} as a vertical uniaxial stress state of the form

$$s = q(x)\, \hat{\boldsymbol{e}}_2 \otimes \hat{\boldsymbol{e}}_2. \tag{21}$$

3.2. ***Membrane form.*** The form of the surface S carrying the compressive membrane stress $\boldsymbol{T}$ can be obtained by studying the transverse equilibrium equation (6). We rewrite such equation in the curvilinear reference (θ^1, θ^2) in the form

$$S^{\alpha\beta} f_{/\alpha\beta} = 0, \tag{22}$$

where $S^{\alpha\beta}$ are the contravariant component of the projected stress in the covariant base $\{\boldsymbol{b}_1, \boldsymbol{b}_2\}$ and the symbol "/" followed by an index, say α, denotes the covariant derivative with respect to the coordinate θ^α.

Differentiating the base vectors and after some algebra, the equation (22) reduces to

$$\frac{q(x)}{1 + y\, g'(\boldsymbol{x})} f_{,22} - p(x, y) = 0, \quad (x, y) \in \Omega_{21}. \tag{23}$$

In the part Ω_{11} the equilibrium equation (23) simplifies to

$$q(x)\, f_{,22}(x, y) - p(x, y) = 0, \quad (x, y) \in \Omega_{11}. \tag{24}$$

This equation can be easily integrated to obtain the shape $f(x, y)$, once $q(x)$ and $p(x, y)$ are given.

3.3. ***Case study:*** **Palazzo Caracciolo di Avellino** ***in Naples.*** The *Palazzo Caracciolo di Avellino*, one of the most ancient monumental buildings of Naples, is located in the Avellino Square and develops along via dell'Anticaglia. It was built at the end of XIV century by the architect Giacomo de Santis, adapting an existent convent as a residence of Gambacorta family. In the late Renaissance, it was inherited by the great poet Torquato Tasso and by the prince Caracciolo di Avellino. The Palace was saved by the destructions of the noble buildings in the revolt of Masaniello against the Spanish viceroyalty. In the XIX century, the edifice was restored and used as condominium. Despite the historical vicissitudes and the changes that have occurred over centuries, the palace is a fine example of Renaissance and Baroque architecture within the historic city of Naples. The Palazzo Caracciolo di Avellino, constituted by two levels with a central courtyard, has recently been undergone to an extensive restoration involving external facades and ground and first floors (see Figure 5).

The form of the surface S carrying the compressive membrane stress $\boldsymbol{T}$ can be obtained by studying the transverse equilibrium equation (24).

In particular, we study the vault 5 (see Figure 5, bottom left). The part of the vault that we analyze is reported in a longitudinal section in Figure 5 (bottom right). The plan of the vault and the partition of the planform into the zones Ω_{21}, Ω_{11}, Ω_{22} and Ω_{12}, are depicted in Figure 6, to which we refer for notations.

Figure 4. *Palazzo Caracciolo di Avellino*: view of the main facade.

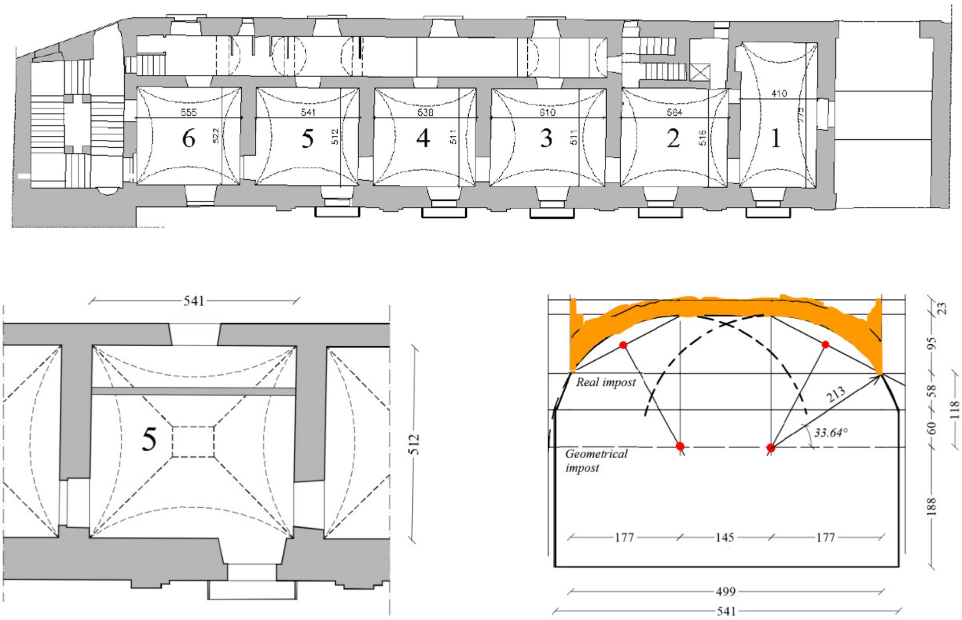

Figure 5. Main facade of the ground floor plan with vaulted structures (top), particular of analyzed cloister vault plan (bottom left) and its longitudinal section (bottom right).

We fix the orientation of the compression rays of Figure 3 (left) by giving (see Figure 7):

$$g(x) = 3\frac{\bar{g}}{l}\left(1 - \frac{4}{3}\frac{x^2}{l^2}\right)x. \tag{25}$$

We consider two types of load. Load 1 is the effect of the dead load in uniform force per unit area $p_0 = 8\,\mathrm{kN/m^2}$, and of the weight w of the wall whose position in the plan is sketched in Figure 5 (top).

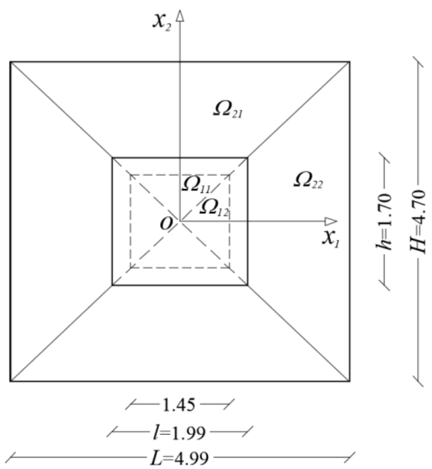

Figure 6. Cloister vault 5: plan dimensions and planform partition zones.

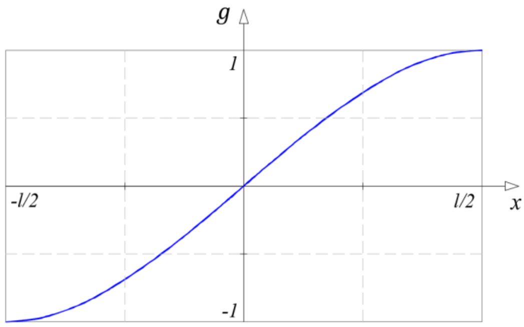

Figure 7. Orientation function (25) of the compressive rays of Figure 3.

As the load w, considering the smearing effect of the filling, we assume the following regularized form:

$$w(x, y) = p_1 \, e^{-\frac{1}{2c}(x-\Delta x)^2} e^{-\frac{1}{2d}(y-\Delta y)^2}, \tag{26}$$

represented in Figure 8 (left).

By solving (23) and (24), the form $f(x, y)$ depicted in Figure 8 (right) is obtained in such a shape contained inside the masonry vault.

Load 2 is the sum of the dead load p_0 and of the load p_{var} representing the effect of a live load. The live load we consider is the weight of a box of water which is 1 m wide, 1 m deep and 0.76 m high. Taking into account the smearing effect of the filling, this load 2 can be sketched as in Figure 9 (left).

As in the previous load case, the shape $f(x, y)$ associated to load 2 and contained inside the masonry vault, is still deducted as solution of equations (26) and (27).

The Heyman geometrical safety factor (see [Heyman 1995; Huerta 2006]), can be assessed by the ratio between the thickness of the real vault and the minimal thickness of a homothetic fictitious vault containing the equilibrium membrane structure S. For both cases of figures 8 (right) and 9 (right), the geometrical safety factor assumes a value near the following:

$$s_H = s/s_{\min} = 20/11 = 1.82. \tag{27}$$

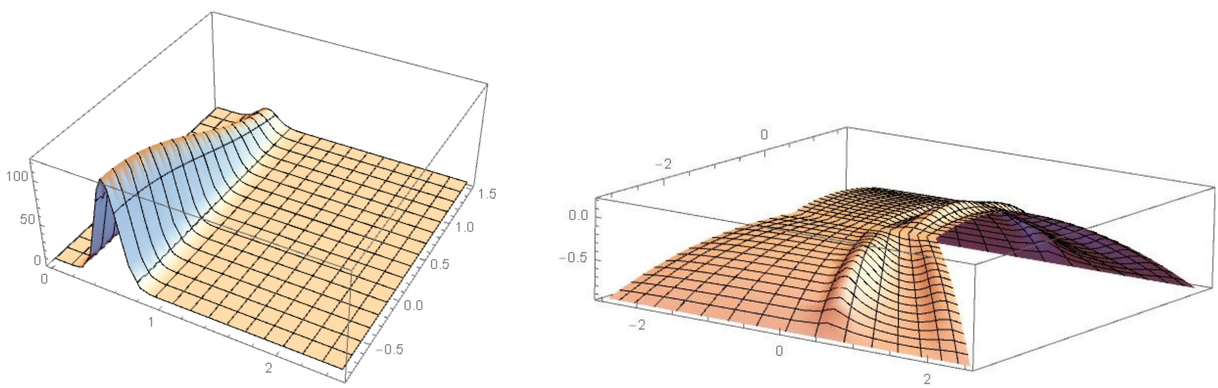

Figure 8. Representation of the load 1 (left) and the form function associated to this load (right).

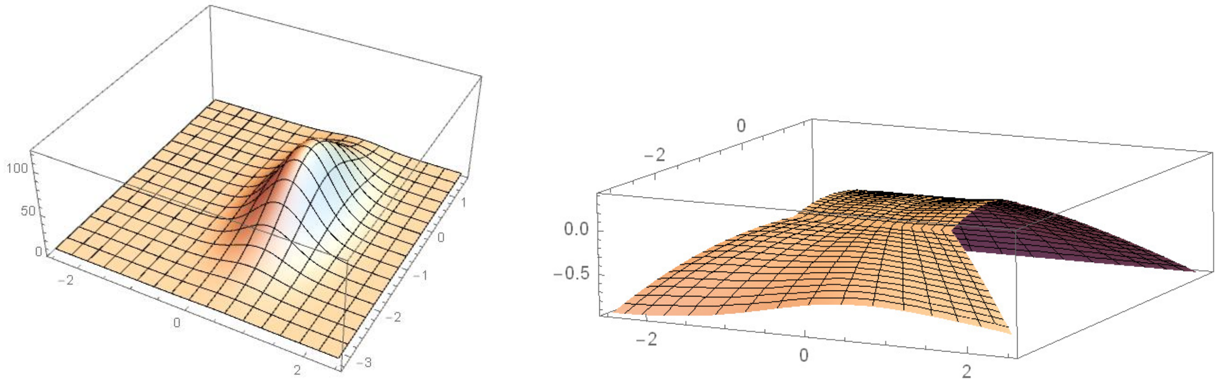

Figure 9. Representation of the load 2 (left) and the form function associated to this load (right).

An upper bound of the collapse load multiplier can be found using the kinematic theorem of limit analysis considering an efficient approach based on the piecewise rigid displacement (PRD) method (see [Iannuzzo et al. 2018c; Iannuzzo et al. 2018b; De Serio et al. 2018]) to adapt at the cloister vault geometry.

4. Concluding remarks

The paper has dealt with the equilibrium of cloister masonry vaults composed of no-tension Heyman material for which the theorems of limit analysis can be still applied. The equilibrium has been expressed as an extension of the Pucher's method, so that convenient systems of coordinates for the formulation of the stress problem and a concave stress function has been assumed. The problem, under purely vertical loads, has turned into a single partial differential equation of the second-order where the shape function f and the stress function F play symmetrical role. The unilateral restrictions have requested that the membrane surface S lies in between the extrados and intrados surfaces of the vault and that the stress function be concave. Making a sensible choice of a concave stress function F, the transverse equilibrium equation has been solved with the unknown function f by imposing suitable boundary conditions. As example, a cloister vault of the *Palazzo Caracciolo di Avellino* has been analyzed, whose membrane surfaces and geometrical safety factors for two load conditions have been assessed.

References

[Angelillo 2015] M. Angelillo, "Static analysis of a Guastavino helical stair as a layered masonry shell", *Compos. Struct.* **119** (2015), 298–304.

[Angelillo 2019] M. Angelillo, "The model of Heyman and the statical and kinematical problems for masonry structures", *Int. J. Masonry Res. Innov.* **4**:1-2 (2019), 14–31.

[Angelillo and Fortunato 2004] M. Angelillo and A. Fortunato, "Equilibrium of masonry vaults", pp. 105–111 in *Novel approaches in civil engineering: lecture notes in applied and computational mechanics*, vol. 14, edited by M. Frémond and F. Maceri, Springer, Berlin, Heidelberg, 2004.

[Angelillo et al. 2010] M. Angelillo, L. Cardamone, and A. Fortunato, "A numerical model for masonry-like structures", *J. Mech. Mater. Struct.* **5**:4 (2010), 583–615.

[Angelillo et al. 2013] M. Angelillo, E. Babilio, and A. Fortunato, "Singular stress fields for masonry-like vaults", *Contin. Mech. Therm.* **25**:2-4 (2013), 423–441.

[Angelillo et al. 2014] M. Angelillo, A. Fortunato, A. Montanino, and M. Lippiello, "Singular stress fields in masonry structures: Derand was right", *Meccanica* (*Milano*) **49**:5 (2014), 1243–1262.

[Angelillo et al. 2016] M. Angelillo, E. Babilio, A. Fortunato, M. Lippiello, and A. Montanino, "Analytic solutions for the stress field in static sandpiles", *Mech. Mater.* **95** (2016), 192–203.

[Angelillo et al. 2018] M. Angelillo, A. Fortunato, A. Gesualdo, A. Iannuzzo, and G. Zuccaro, "Rigid block models for masonry structures", *Int. J. Masonry Res. Innov.* **3**:4 (2018), 349–368.

[Bloch and Ochsendorf 2007] P. Bloch and J. Ochsendorf, "Thrust network analysis: a new methodology for three-dimensional equilibrium", *J. IASS* **48**:3 (2007), 167–173.

[Block and Lachauer 2014] P. Block and L. Lachauer, "Three-dimensional funicular analysis of masonry vaults", *Mech. Res. Commun.* **56** (2014), 53–60.

[Block et al. 2006] P. Block, T. Ciblac, and J. Ochsendorf, "Real-time limit analysis of vaulted masonry buildings", *Comput. Struct.* **84**:29-30 (2006), 1841–1852.

[Brandonisio et al. 2013] G. Brandonisio, G. Lucibello, and A. Mele, E. De Luca, "Damage and performance evaluation of masonry churches in the 2009 L'Aquila earthquake", *Eng. Fail. Anal.* **34** (2013), 693–714.

[Brandonisio et al. 2015] G. Brandonisio, E. Mele, and A. De Luca, "Closed form solution for predicting the horizontal capacity of masonry portal frames through limit analysis and comparison with experimental test results", *Eng. Fail. Anal.* **55** (2015), 246–270.

[Como 1992] M. Como, "Equilibrium and collapse analysis of masonry bodies", *Meccanica* (*Milano*) **27**:3 (1992), 185–194.

[Como 2013] M. Como, *Statics of historic masonry constructions*, Springer, Berlin, 2013.

[Contestabile et al. 2016] M. Contestabile, E. Babilio, A. Fortunato, L. Guerriero, M. Lippiello, M. Pasquino, and M. Angelillo, "Static analysis of cross vaults: the case of the cathedral of Casertavecchia", *Open Construct. Build. Technol. J.* **10**:Suppl 2: M11 (2016), 329–345.

[De Goes et al. 2013] F. De Goes, P. Alliez, H. Owhadi, and M. Desbrun, "On the equilibrium of simplicial masonry structures", *ACM Trans. Graph.* **32**:4 (2013), article 93.

[De Serio et al. 2018] F. De Serio, M. Angelillo, A. Gesualdo, A. Iannuzzo, G. Zuccaro, and M. Pasquino, "Masonry structures made of monolithic blocks with an application to spiral stairs", *Meccanica* (*Milano*) **53**:8 (2018), 2171–2191.

[Fang et al. 2019] D. L. Fang, R. K. Napolitano, T. L. Michiels, and S. M. Adriaenssens, "Assessing the stability of unreinforced masonry arches and vaults: a comparison of analytical and numerical strategies", *Int. J. Archit. Herit.* **13**:5 (2019), 648–662.

[Fortunato et al. 2014] A. Fortunato, F. Fraternali, and M. Angelillo, "Structural capacity of masonry walls under horizontal loads", *Ing. Sismica* **31**:1 (2014), 41–49.

[Fortunato et al. 2016] A. Fortunato, E. Babilio, M. Lippiello, A. Gesualdo, and M. Angelillo, "Limit analysis for unilateral masonry-like structures", *Open Construct. Build. Technol. J.* **10**:Suppl 2: M12 (2016), 346–362.

[Fortunato et al. 2018] A. Fortunato, F. Fabbrocino, M. Angelillo, and F. Fraternali, "Limit analysis of masonry structures with free discontinuities", *Meccanica* (*Milano*) **53**:7 (2018), 1793–1802.

[Fraternali 2010] F. Fraternali, "A thrust network approach to the equilibrium problem of unreinforced masonry vaults via polyhedral stress functions", *Mech. Res. Commun.* **37**:2 (2010), 198–204.

[Fraternali et al. 2002] F. Fraternali, M. Angelillo, and G. Rocchetta, "On the stress skeleton of masonry vaults and domes", in *Proceedings of the Seventh Pan American Congress of Applied Mechanics (PACAM VII)* (Temuco, Chile), 2002.

[Gesualdo et al. 2017] A. Gesualdo, C. Cennamo, A. Fortunato, G. Frunzio, M. Monaco, and M. Angelillo, "Equilibrium formulation of masonry helical stairs", *Meccanica* (*Milano*) **52**:8 (2017), 1963–1974.

[Gesualdo et al. 2019] A. Gesualdo, B. Calderoni, A. Sandoli, and M. Monaco, "Minimum energy approach for the in-plane shear resistance of masonry panels", *Ing. Sismica* **36**:1 (2019), 42–53.

[Heyman 1966] J. Heyman, "The stone skeleton", *Int. J. Solids Struct.* **2**:2 (1966), 249–279.

[Heyman 1995] J. Heyman, *The stone skeleton: structural engineering of masonry architecture*, Cambridge University Press, Cambridge, UK, 1995.

[Heyman 2012] J. Heyman, "The membrane analysis of thin masonry shells", *Nuts Bolts Construct. Hist.* **1** (2012), 281–283.

[Huerta 2006] S. Huerta, "Galileo was wrong: the geometrical design of masonry arches", *Nexus Netw. J.* **8**:2 (2006), 25–52.

[Iannuzzo et al. 2018a] A. Iannuzzo, M. Angelillo, E. De Chiara, F. De Guglielmo, F. De Serio, F. Ribera, and A. Gesualdo, "Modelling the cracks produced by settlements in masonry structures", *Meccanica* (*Milano*) **53**:7 (2018), 1857–1873.

[Iannuzzo et al. 2018b] A. Iannuzzo, A. De Luca, A. Fortunato, A. Gesualdo, and M. Angelillo, "Fractures detection in masonry constructions under horizontal seismic forces", *Ing. Sismica* **35**:3 (2018), 87–103.

[Iannuzzo et al. 2018c] A. Iannuzzo, F. De Serio, A. Gesualdo, G. Zuccaro, and M. Fortunato, A. Angelillo, "Crack patterns identification in masonry structures with a C^0 displacement energy method", *Int. J. Masonry Res. Innov.* **3**:3 (2018), 295–323.

[Kooharian 1952] A. Kooharian, "Limit analysis of voussoir (segmental) and concrete arches", *J. Am. Concr. Inst.* **24**:4 (1952), 317–328.

[Livesley 1978] R. K. Livesley, "Limit analysis of structures formed from rigid blocks", *Int. J. Numer. Methods Eng.* **12**:12 (1978), 1853–1871.

[Marmo and Rosati 2017] F. Marmo and L. Rosati, "Reformulation and extension of the thrust network analysis", *Comput. Struct.* **182** (2017), 104–118.

[Miki et al. 2015] M. Miki, T. Igarashi, and P. Block, "Parametric self-supporting surfaces via direct computation of airy stress functions", *ACM Trans. Graph.* **34**:4 (2015), article 89.

[O'Dwyer 1999] D. W. O'Dwyer, "Funicular analysis of masonry vaults", *Comput. Struct.* **73**:1-5 (1999), 187–197.

[Pucher 1934] A. Pucher, "Über der spannungszustand in gekrümmten flächen", *Beton u Eisen* **33** (1934), 298–304.

[Vouga et al. 2012] E. Vouga, M. Höbinger, J. Wallner, and H. Pottmann, "Design of self-supporting Surfaces", *ACM Trans. Graph.* **31**:4 (2012), article 87.

Received 11 Apr 2019. Revised 11 Oct 2019. Accepted 28 Oct 2019.

ANTONIO GESUALDO: gesualdo@unina.it
Department of Structures for Engineering and Architecture, University of Naples Federico II, Via Claudio 21 (buildings 6-7), 80125 Naples, Italy

GIUSEPPE BRANDONISIO: giuseppe.brandonisio@unina.it
Department of Structures for Engineering and Architecture (Di.St.), University of Naples "Federico II", P.le Tecchio, 80, 80125 Naples, Italy

ANTONELLO DE LUCA: antonio.deluca@unina.it
Department of Structures for Engineering and Architecture (Di.St.), University of Naples "Federico II", P.le Tecchio, 80, 80125 Naples, Italy

ANTONINO IANNUZZO: iannuzzo@arch.ethz.ch
Institute of Technology in Architecture, Block Research Group, ETH Zurich, Stefano-Franscini-Platz 1, 8093 Zurich, Switzerland

ANDREA MONTANINO: andrea.montanino@polimi.it
Dipartimento di Strutture per L'Ingegneria e l'Architettura, Universita degli studi di Napoli "Federico II", Via Toledo, 902, 80132 Napoli, Italy

CARLO OLIVIERI: colivieri@unisa.it
Department of Civil Engineering, University of Salerno, Via Giovanni Paolo II, 132, 84084 Fisciano, Italy

JOURNAL OF MECHANICS OF MATERIALS AND STRUCTURES

msp.org/jomms

Founded by Charles R. Steele and Marie-Louise Steele

Cover photo: Mando Gomez, www.mandolux.com

See msp.org/jomms for submission guidelines.

JoMMS (ISSN 1559-3959) at Mathematical Sciences Publishers, 798 Evans Hall #6840, c/o University of California, Berkeley, CA 94720-3840, is published in 10 issues a year. The subscription price for 2019 is US $635/year for the electronic version, and $795/year (+$60, if shipping outside the US) for print and electronic. Subscriptions, requests for back issues, and changes of address should be sent to MSP.

JoMMS peer-review and production is managed by EditFlow® from Mathematical Sciences Publishers.

PUBLISHED BY

mathematical sciences publishers

nonprofit scientific publishing

http://msp.org/

Journal of Mechanics of Materials and Structures

Volume 14, No. 5 December 2019